Current Science
CS 5 (4), 4134-4148 (2025)
Received 13 May 2025 | **Revised 12 June** 2025 | **Accepted 17 July**. 2025 | **Online Available 27 August** 2025
https://doi.org/ 10.52845/CS/2025-5-4-62

Current Science
Current Science

OPEN ACCESS

ISSN(O)2795-8639

Original Article

Simulation Study of Electron Beam Process Parameters on EB Furnace Melting Raw Materials

Hang Ran[1,2], Yu Liu[1], Junhao Xiao[1], Bing Zhao[1*]

[1]School of Mechanical Engineering, Qinghai University, Xining 810016, Qinghai, People's Republic of China

[*]Corresponding Author: Bing Zhao

Abstract:
In the process of melting titanium alloys in electron beam cold hearth melting furnace, the process parameters of electron beam are crucial to the melting rate of titanium alloys. In view of the influence of electron beam process parameters on the melting rate, the finite element method was used to calculate and analyze the melting process of titanium alloy in EB furnace in detail, and the change of raw material temperature field under different process parameters of electron beam was studied. The results show that increasing the scanning speed of the electron beam significantly reduces the melting depth and width. Increasing the diameter of the electron beam deepens and widens the melting depth. Widening the scan spacing can slightly reduce the melting depth, but significantly broaden the melting width. The accelerating voltage and the current emitted by the electron beam have a limited effect on the melting due to their thermal saturation effect. Furthermore, this study provides theoretical support for the optimization of electron beam process parameters for electron beam cold hearth melting of titanium alloys, and the optimization strategy needs to be combined with parameter adjustments to improve the efficiency of single melting and reduce the number of scans.

1. Introduction

Electron Beam Cold Hearth Melting (EBCHM) uses an electron beam as the heat source, and the melting of raw materials is achieved by bombarding the raw materials to be melted by high-speed electron beams, so that the kinetic energy of electrons is converted into heat energy. Electron Beam Melting (EBM) is an advanced metal additive manufacturing technology with core advantages such as high precision, high material utilization, excellent material properties, shortened production cycle, suitable for a variety of metal materials, reduced subsequent processing needs, high automation and digitalization, suitable for small batch customized production, environmental protection and sustainability, and reduced inventory and logistics costs[1,2]. These advantages make electron beam melting technology have a wide range of application prospects in aerospace, medical, automotive and other fields, and is expected to become one of the important technologies in the field of metal manufacturing in the future. Electron Beam Melting (EBM) technology: In the melting process of the electron beam cold hearth melting furnace, it is not only able to melt the alloy, but also remove low-density inclusions on the surface of the cold hearth through the high temperature of the electron beam[3].

Electron Beam Melting Technology is the most widely used high-purity (4N5 and above) refining technology for rare metals; This is because the method allows impurities to volatilize rapidly by transferring energy to the surface by pure thermoelectricity under ultra-vacuum conditions. Although the electron beam in the EBM process is applied at a constant power, the energy density absorbed by the molten material fluctuates depending on the spot area due to the focus of the

electron beam. When the electron beam is focused on the surface of the molten material, its energy distribution changes to a Gaussian distribution, with the highest density in the center.

In order to more clearly reveal the influence of different electron beam parameters on the melting of raw materials in the melting process of EB furnace, many researchers have studied the electron beam melting process. L GAO[4] simulated the process of melting TC4 titanium alloy in EB furnace through Fluent software, and studied the temperature change of the molten pool under the reciprocating scanning heating of electron beam. Körner C[5] discusses the mechanism by which the power, scanning speed and spot size of the electron beam affect the melting process and the properties of the material. L Cao[6] studied the changes in surface morphology, density, microstructure and mechanical properties of electron beam melting samples under different accelerating voltages. Hongxin L[7] studied the changes in solidification morphology under different temperature gradients and electron beam scanning rates, and the results showed that when the ratio of temperature gradient to scanning rate decreased, the solidification morphology gradually changed from flat crystals to honeycomb crystals, columnar crystals, and even dendritic structures. The influence of the electron beam on the properties of the material was studied, and the temperature field of the raw material melting process was rarely described, and then the electron beam parameters (electron beam scanning speed, diameter, acceleration voltage, current and scanning spacing) were studied to simulate the melting TC4 titanium alloy in the EB furnace[8].

Principles and Methods

The Working Principle of the Electron Gun

The electron beam is generated by the electron gun, and the electron gun is divided into cold cathode electron gun and hot cathode electron gun by the difference of cathode, the hot cathode is heated cathode to excite electrons, and the cold cathode is generally excited by an externally strengthened electric field. In contrast, the cold cathode electron gun does not need to be heated when working, and the efficiency is higher than that of the hot cathode electron gun, and the cold cathode electron gun also solves the problems of large volume, high power consumption and low response of the hot cathode electron gun, so it has greater advantages[9,10]. The cathode is generally made of aluminum alloy, this is because (1) the working temperature of the cold cathode electron gun is low, the cold cathode does not need to be heated to a high temperature to emit electrons, and the aluminum alloy as a cathode material can work at a relatively low temperature, which can reduce energy consumption and simplify the design of the electron gun; (2) Aluminum alloy can produce high electron emission current density at a lower electric field; (3) Aluminum alloy has good corrosion resistance, and can resist oxidation and other chemical corrosion in the working environment of the electron gun, thereby prolonging the service life; (4) Aluminum alloy has good machinability and can be easily processed into the required shape and size, which is conducive to the manufacture of electron guns; (5) The thermal conductivity of aluminum alloy is high, which is conducive to the rapid dissipation of heat on the surface of the cathode, which is very beneficial to maintaining the low temperature working state of the cathode; (6) The density of aluminum alloy is low, which can reduce the weight of the entire electron gun; (7) Aluminum alloys can more easily achieve electron emission through proper treatment (such as coating materials with low escape work materials or using special alloy compositions). However, aluminum alloy cold cathodes also have their limitations, such as the emission stability may not be as good as that of hot cathodes, and the material aging problems that may occur after long-term use. Therefore, when selecting the cathode material of the electron gun, it is necessary to comprehensively consider its advantages and disadvantages as well as the needs of specific application scenarios.

The structure of the cold cathode electron gun is relatively simple, mainly composed of a cathode, an anode, two focusing coils and a deflection coil, and its structure is shown in Fig. 1. When starting the electron gun, it is necessary to pass in the working gas (high-purity hydrogen), the hydrogen glow discharge occurs under DC high voltage, the plasma emission generated under the glow discharge condition accelerates through the electric field in the cathode potential drop region, bombards the aluminum alloy cathode, and when the continuous bombardment reaches the

minimum escape work, the metal electrons will overcome the binding force on the metal surface, escape from the cathode surface, produce secondary electrons, and under the acceleration of the electric field at the two poles, a converging electron beam through the focusing and scanning system in the middle of the anode is formed; The magnetic field of the first focusing coil forms an approximately cylindrical electron beam with no loss of power; Then, the magnetic field of the second focusing coil changes the direct heating area of the electron beam. Process-specific electron beam scanning by means of a deflection coil.

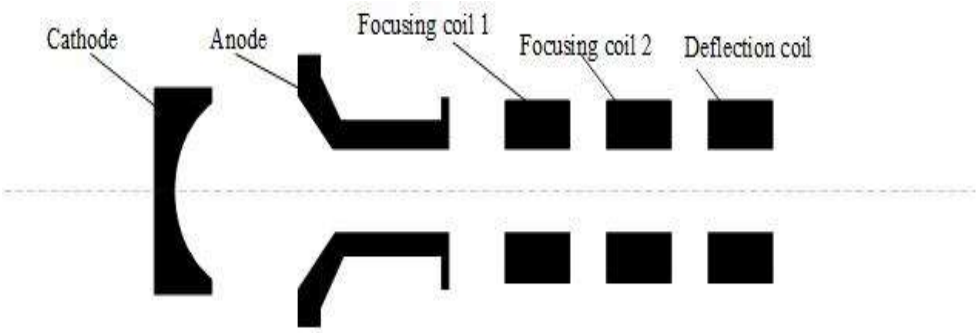

Fig. 1. Structure diagram of electron gun

In the process of operating the aluminum alloy cold cathode electron beam gun, when the hydrogen flow is large enough and the cathode reaches a certain temperature, the current is difficult to increase, the electron gun chamber is provided with mixed working gas (hydrogen and oxygen are mixed in a certain proportion), and the oxygen ions are accelerated in the electric field, bombarding the cathode, and playing the role of cleaning the surface of the cathode, thereby increasing the current.

The melting speed of the electron beam melting raw material is closely related to the relevant parameters of the electron beam (such as the scanning speed, diameter, accelerating voltage, current and scanning spacing) of the electron beam cold hearth. The faster smelting of raw materials can reduce the time it takes to melt titanium ingots and speed up the production process of titanium ingots. Therefore, it is of great significance to explore the relationship between the process parameters and the temperature field of the electron beam for the production process of titanium ingots.

Temperature Field Control Model

- Considering the process of electron beam melting TC4 titanium alloy, the electron beam scans the surface of the titanium alloy, and the titanium alloy absorbs the energy released by the electron beam, which increases the temperature of the titanium alloy. The lower left corner of the titanium alloy surface is set as the origin of the three-dimensional Cartesian coordinate system (x, y, z), as shown in Fig. 2. The melting process of titanium alloys involves complex heat transfer, which can be represented by the Fourier thermal conductivity partial differential equation, which is:

$$\rho(T)c(T)\frac{\partial T}{\partial t} = \nabla \cdot [\lambda(T)\nabla T] + Q \quad (1)$$

Where $\nabla = \frac{\partial i}{\partial t} + \frac{\partial j}{\partial t} + \frac{\partial k}{\partial t}$($i$, j , k represent the unit vectors of the x, y, z, respectively)，Q represents the internal heat source; ρ is the density of titanium alloy; c is the specific heat capacity of constant pressure; λ is the thermal conductivity; ρ, c, λ are all functions of temperature T.

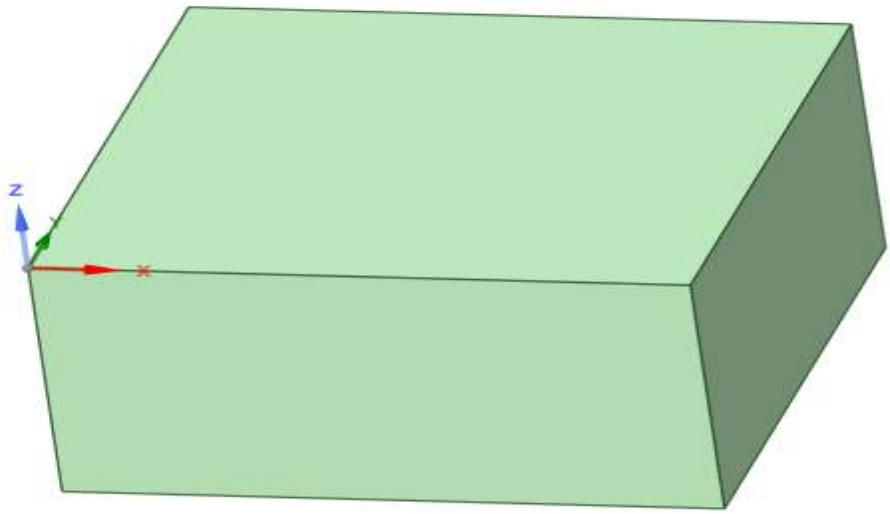

Fig. 2. Raw material coordinate diagram

When the temperature is in the two-phase zone (paste zone),

$$Q = \rho L \frac{\partial F_S}{\partial t} \quad (2)$$

Where L is the latent heat of coagulation，F_s is the solid-phase ratio。

When the temperature is higher than the liquidus temperature or lower than the solidus temperature, the internal heat source Q=0.

Heat Source Model

The heat source model is the basis of the temperature field simulation, which directly determines the accuracy of the entire simulation process. In order to simulate the temperature field distribution, the Gaussian surface heat source is selected for the electron beam model, and its intensity in the horizontal and vertical directions obeys the Gaussian distribution[11]. The model diagram is shown in Fig. 3.

$$q(r) = \frac{3\eta UI}{\pi R^2} \exp(-\frac{3r^2}{R^2}) \quad (3)$$

where q is the energy density of the electron beam; η is the energy conversion efficiency of the electron beam, generally 0.75~0.95, and U is the accelerating voltage (kv); I is the electron beam current (A); r is the distance between the heating node and the center of the heat source (mm), $r = \sqrt{(x-a)^2 + (y-b)^2}$ (x, y) is the coordinate of the heating node, and (a, b) is the coordinate of the center of the heat source; R is the electron beam spot radius (mm).

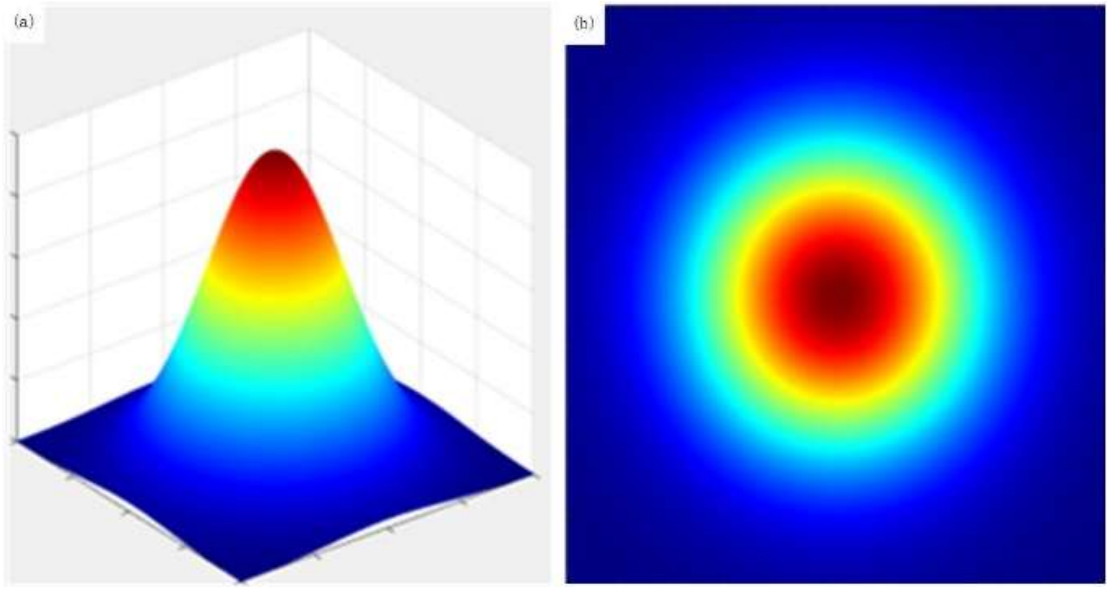

Fig. 3. Model diagram of electron beam heat source (a) Horizontal (b) Vertical

The heat source is a moving heat source, the moving speed is v(mm/s), and the moving trajectory of the heat source is shown in Fig. 4.

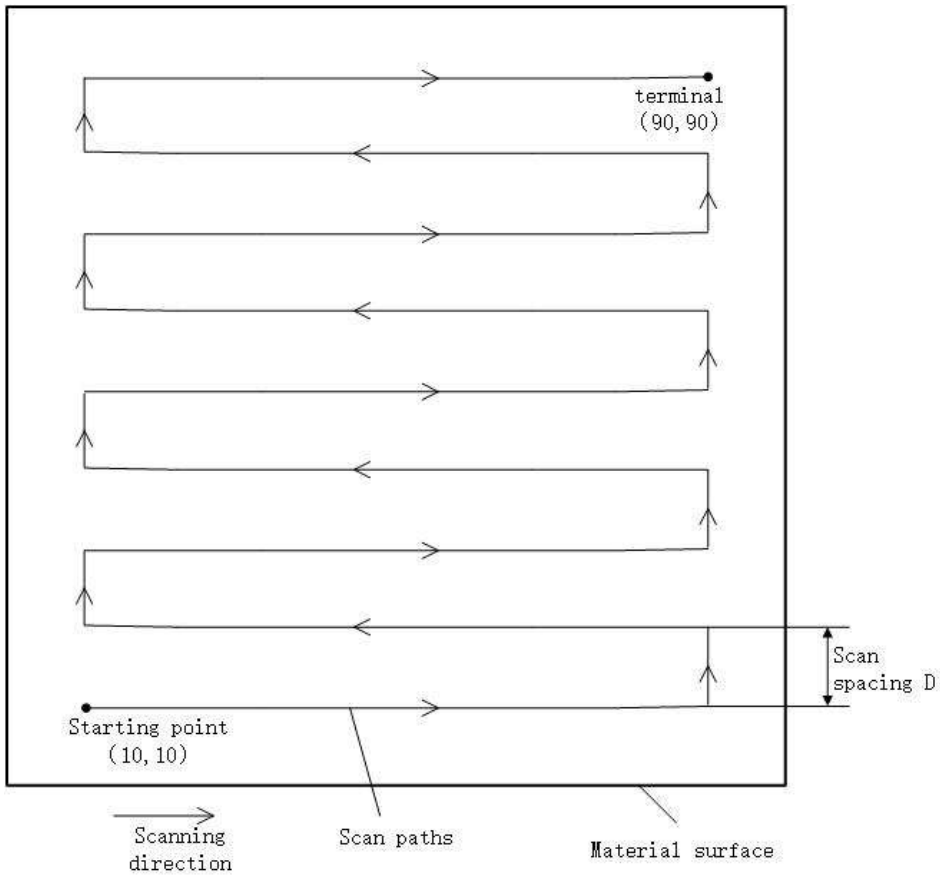

Fig. 4. Electron beam scanning path

Boundary Conditions

The simulated boundary conditions of the electron beam melting process of TC4 titanium alloy mainly include heat conduction, heat convection, heat radiation and latent heat. The following initial conditions and boundary conditions are assumed, assuming that the initial temperature of electron beam melting TC4 is room temperature:

$$T|_{t=0} = T_0 \quad (4)$$

where T0 is the initial temperature and the simulated room temperature is 300 K.

The heat transfer during the melting process of TC4 titanium alloy can be expressed as:

$$-k\frac{\partial T}{\partial z} = a(T - T_0) \quad (5)$$

where a is the thermal conductivity of the TC4 titanium alloy and T is the current temperature (K).

Because the smelting process is in a high vacuum state, the air is relatively thin, so no convection heat exchange is set, and surface heat radiation heat release is set, and the specific radiation heat release is shown in the formula.

$$q_R = -A \cdot \sigma \cdot \varepsilon (T^4 - T_0^4) \quad (6)$$

where A is the radiant surface area and σ is the Stefan-Boltzmann constant, which is about 5.67×10^{-8} W/($m^2\cdot K^4$); ε=0.2 is the emissivity.

Geometric Modeling and its Meshing

A geometric model of the TC4 titanium alloy (with dimensions of 100×100×50 mm) was created using a 3D modeling tool and imported into ANSYS finite element software for meshing, as shown in Fig. 5. In the analysis of the results of electron beam melting TC4, the influence of electron beam parameters on the temperature and melting depth of the raw material surface was mainly studied.

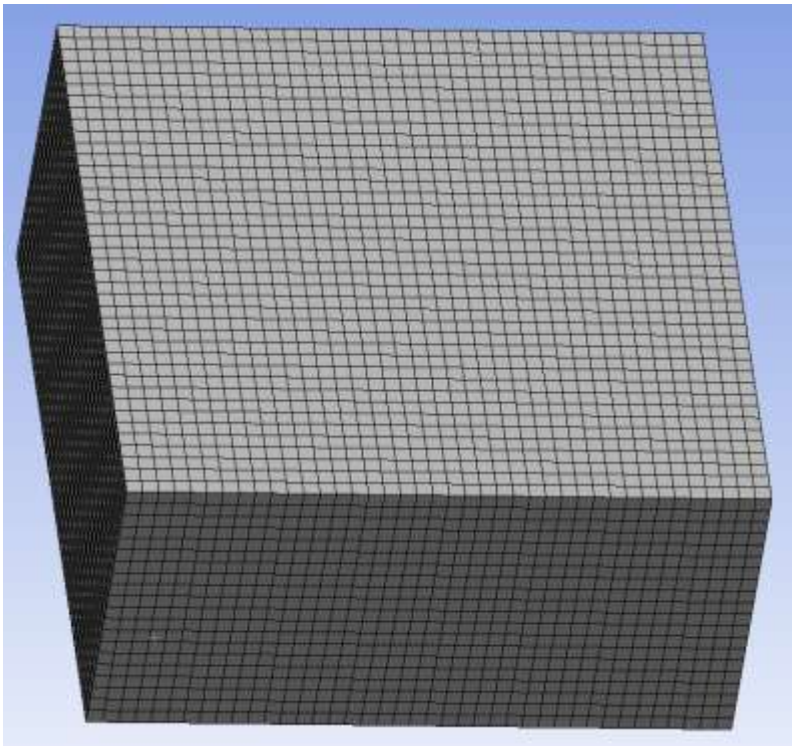

Fig. 5. Meshing diagram

Results and Discussion

In the finite element model, the electron beam is simulated by the Gaussian heat source of Eq. 3, the UDF (custom function) is written by combining Fluent-specific macros in C language, the UDF is loaded on the upper surface of the raw material for operation, the process parameters of

the Gaussian heat source are changed through the UDF[12], and the temperature changes of the plane of y=10+D mm and the upper surface of the raw material are studied when the midpoint of the electron beam moves to the (50, 10+D) point under different electron beam process parameters.

When the temperature is above the solidus line, the raw material begins to melt; When the temperature is higher than the liquidus line, the raw material is completely melted into a liquid, as shown in **Error! Reference source not found.**.

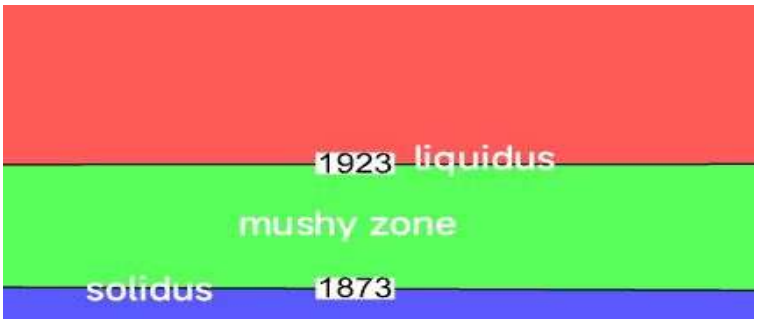

Fig. 6. Solid-liquid phase illustration diagram

The distance from the upper surface to the solidus is the melting depth, as shown in Fig. 7a; The distance from the front surface to the solidus is the melting width, as shown in Fig. 7b.

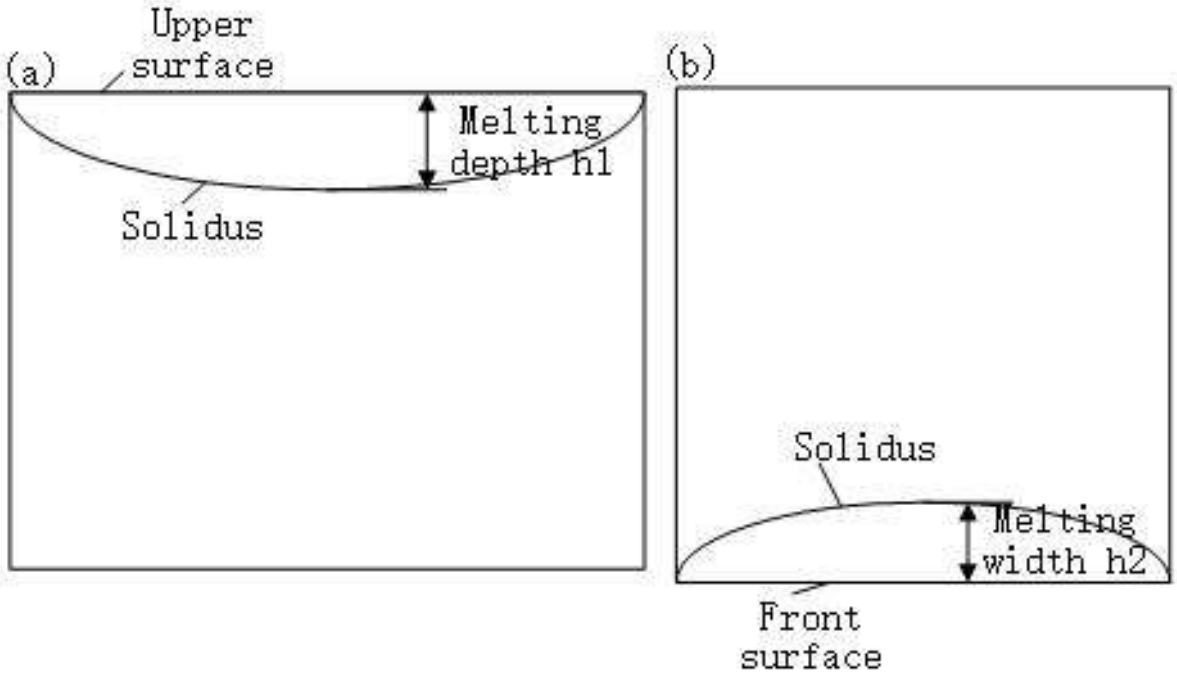

Fig. 7.Raw material melting diagram (a)Melting depth (b)Melting width

Effect of Electron Beam Scanning Speed on TC4 Melting Process

In order to study the influence of different scanning speeds[13] of the electron beam on the surface temperature field of the titanium alloy and the change of the melting depth of the titanium alloy during the smelting process, the temperature change of y=20mm plane (D=10mm) when the scanning speed of the electron beam is 10mm/s, 20mm/s, 40mm/s, and the midpoint of the electron beam moves to the (50, 20) point, , respectively. And other process parameters of the electron beam used in the simulation are shown in

Table **I**:

Table I. Process parameters

Scanning speed	Electron beam	Voltage	Current	Scanning

v(mm/s)	diameter d(mm)	U(kv)	I(A)	spacing D(mm)
—	10	30	5	10

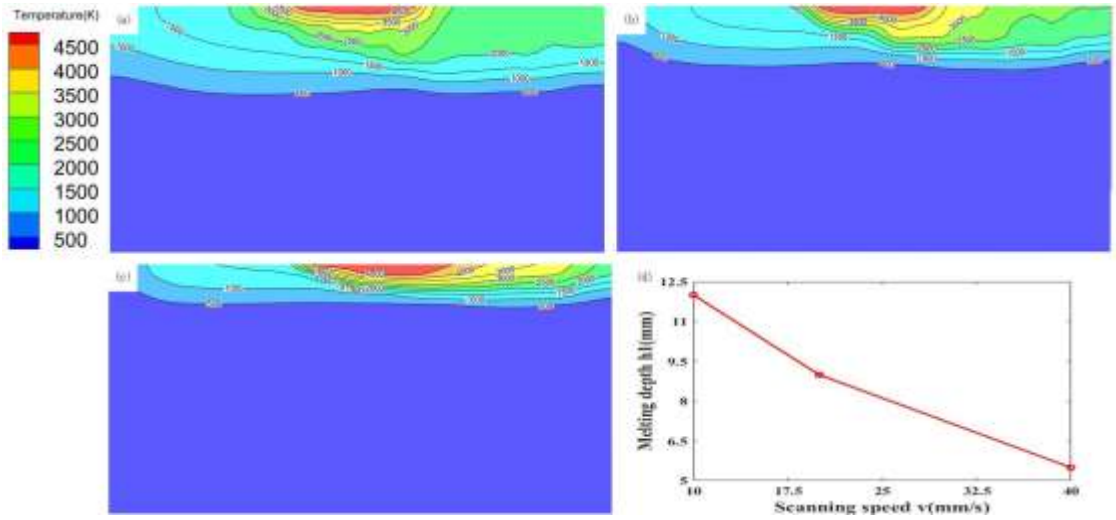

Fig. 8. Temperature graph of y=20 mm plane (a)v=10mm/s (b)v=20mm/s (c)v=40mm/s

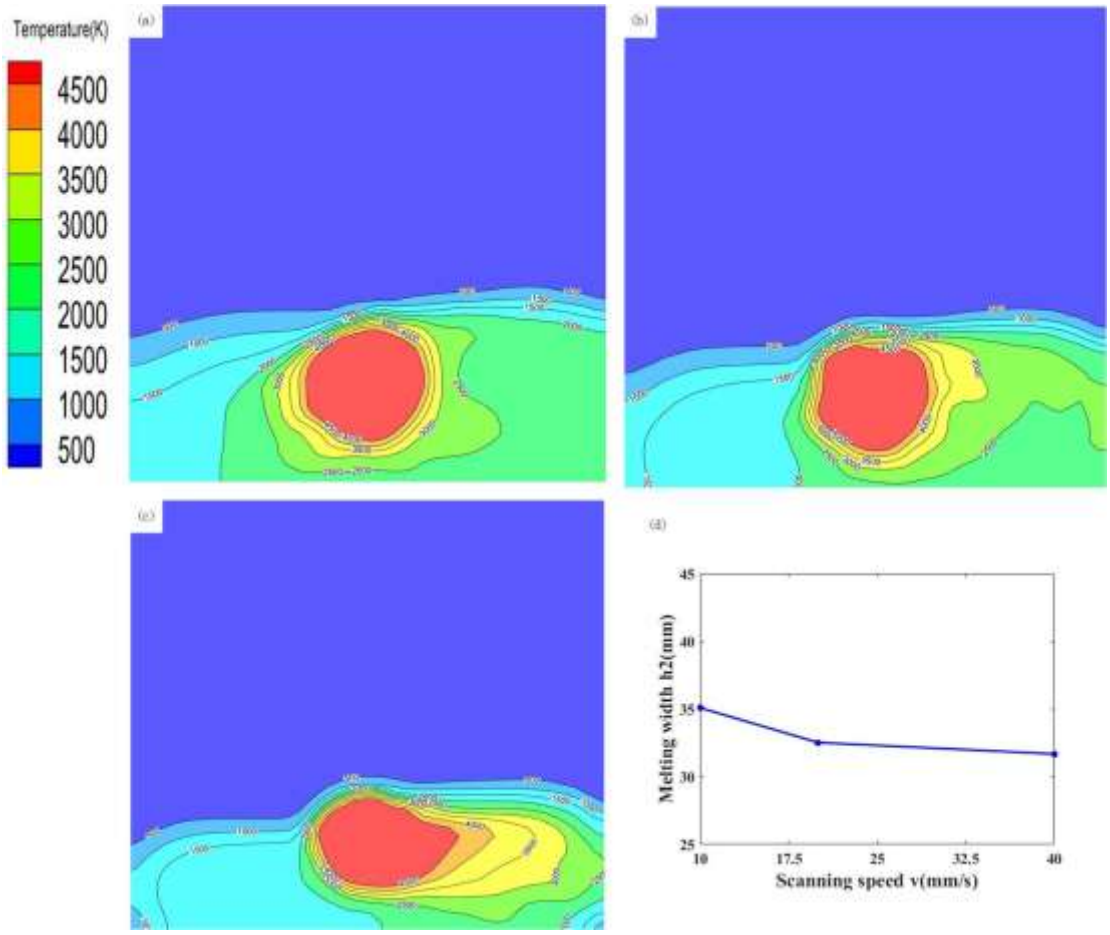

Fig. 9. Upper surface temperature map (a)v=10mm/s (b)v=20mm/s (c)v=40mm/s

Table II. Relationship between scanning speed and melting

Scanning speed v（mm/s）		10		20		40
Melting depth h1（mm）		12.20		8.99		5.49
Melting width h2（mm）		35.09		32.52		31.68

Under the condition that other conditions remain constant, increasing the scanning speed of the electron beam and observing the temperature field change of the titanium alloy, it can be concluded from Fig. 8,Fig. 9 and

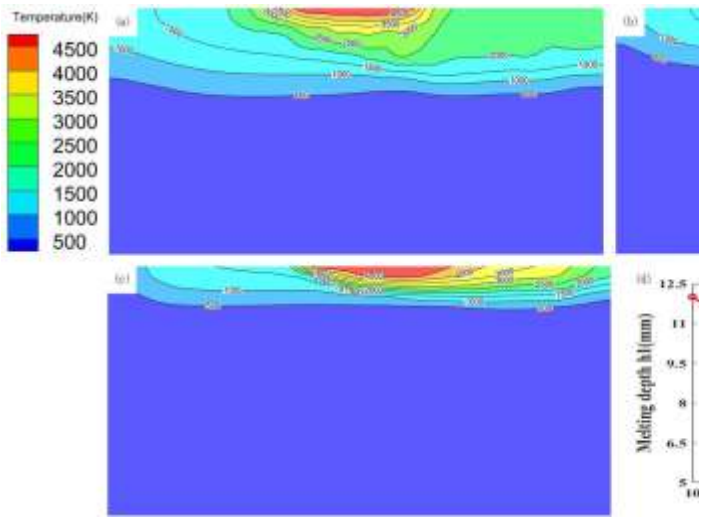

Fig. 8. Temperature graph of y=20 mm plane (a)v=10mm/s (b)v=20mm/s (c)v=40mm/s

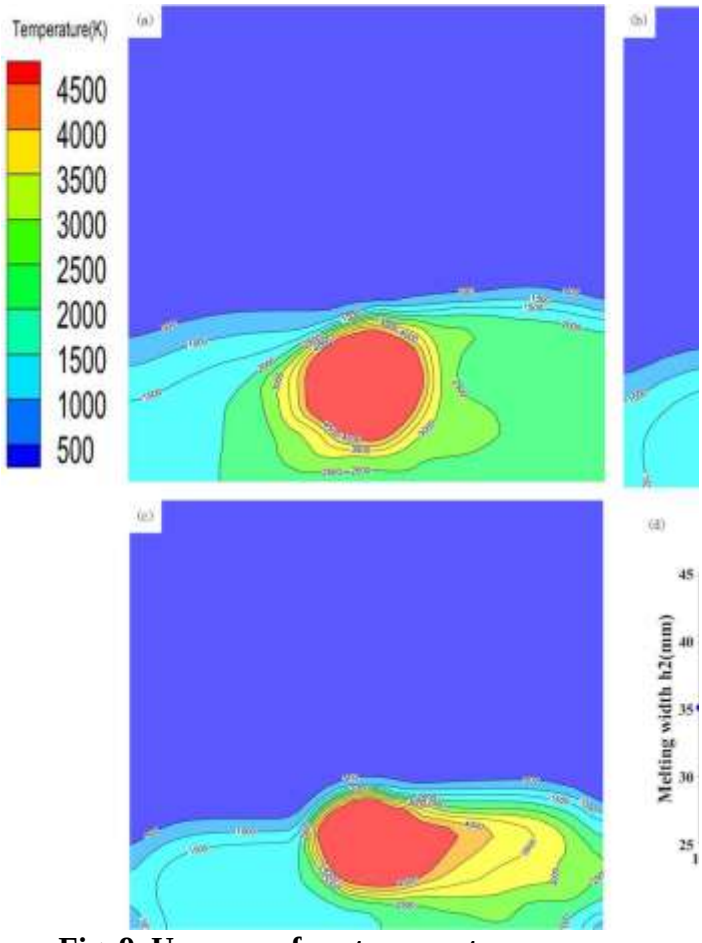

Fig. 9. Upper surface temperature map (a)v=10mm/s (b)v=20mm/s (c)v=40mm/s

Table II that the acceleration of the scanning speed of the electron beam will gradually make the melting depth gradually shallower and the melting width gradually narrower. When the scanning speed is increased from 10 mm/s to 40 mm/s, the melting depth is reduced from 12.20 mm to 5.49 mm, indicating that a reasonable slowdown in the scanning speed can make the raw material melt quickly and reduce the number of scans.

Effect of Electron Beam Diameter on TC4 Melting Process

In order to study the influence of different electron beam diameters[14] on the surface temperature field and the change of melting depth of titanium alloy during the melting process of titanium alloy, the temperature change of y=20mm plane (D=10mm) when the diameter of the electron beam is 10mm, 20mm, 40mm, and when the midpoint of the electron beam moves to the (50, 20) point, respectively. And other process parameters of the electron beam used in the simulation are shown in Table III:

Table III. Process parameters

Scanning speed	Electron beam	Voltage U(kv)	Current	Scanning

v(mm/s)	diameter d(mm)		I(A)	spacing D(mm)
20	—	30	5	10

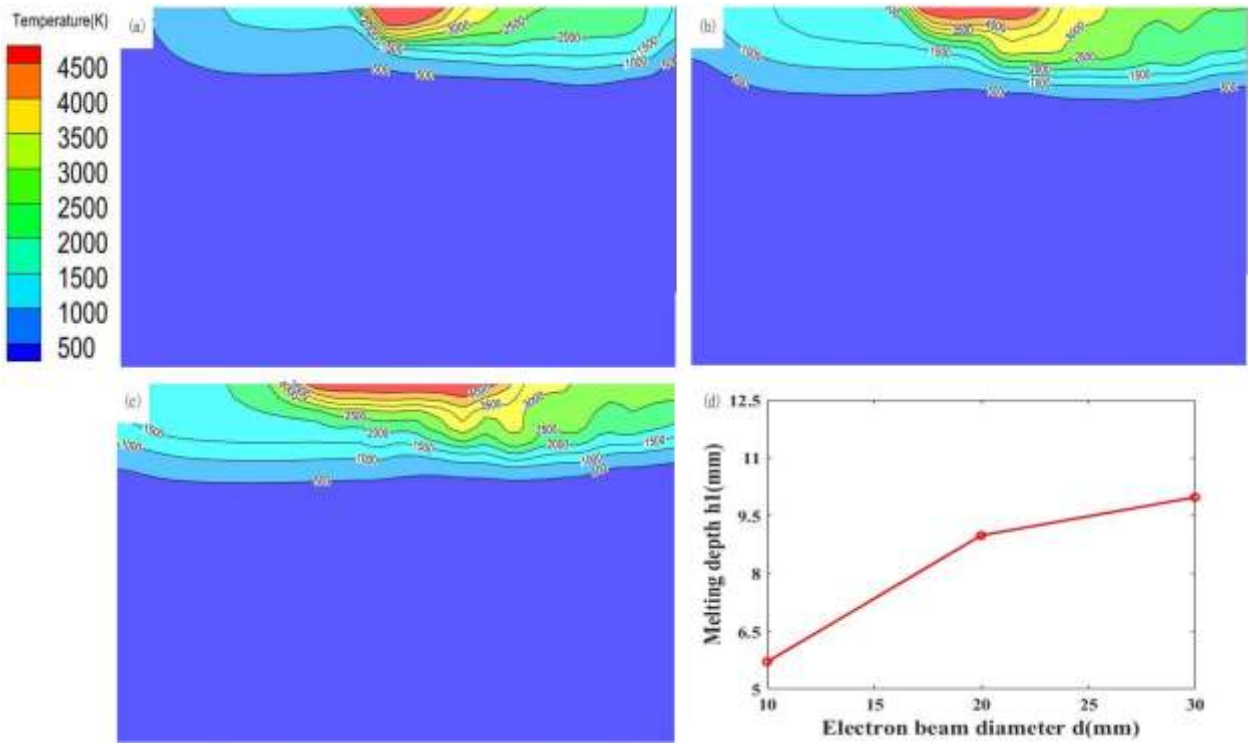

Fig. 10. Plane temperature diagram of y=20 mm (a)d=10mm (b)d=20mm (c)d=30mm

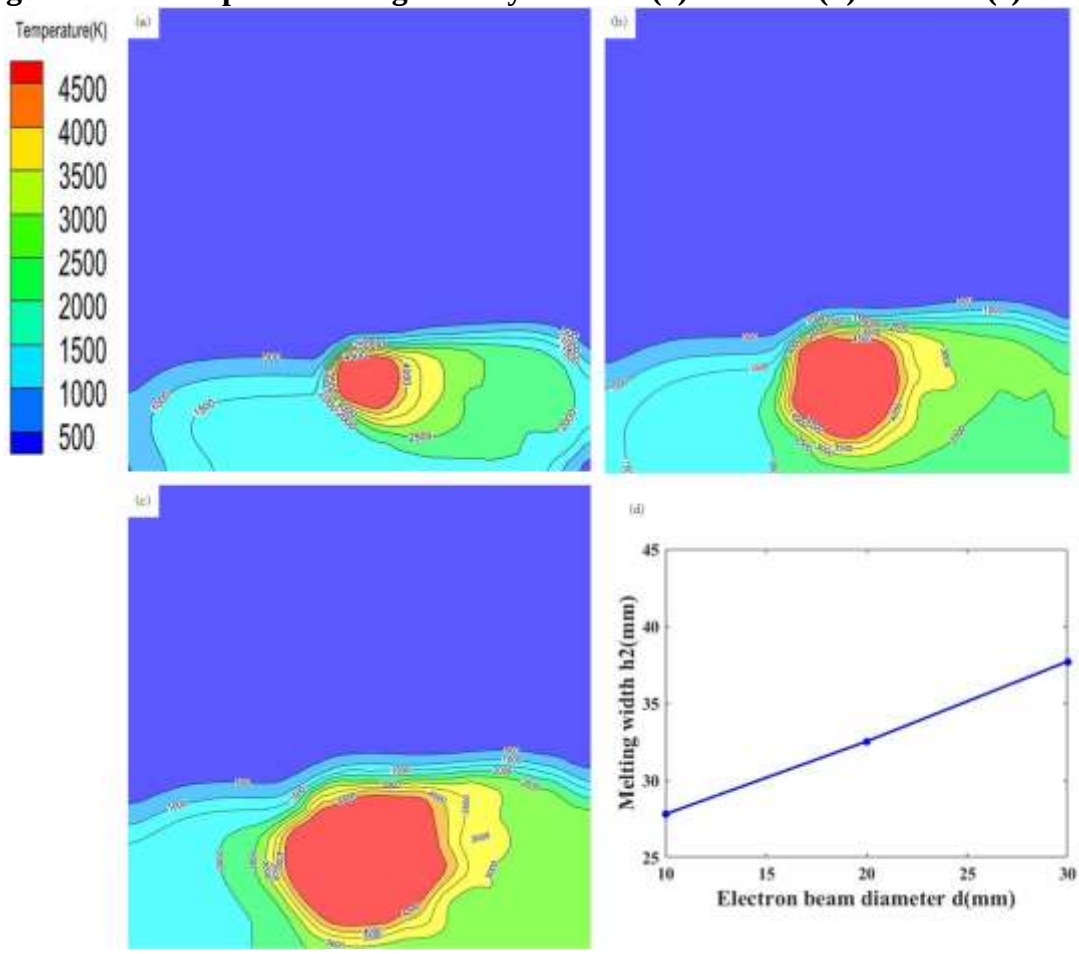

Fig. 11. Upper surface temperature map (a)d=10mm (b)d=20mm (c)d=30mm

Table IV. Relationship between electron beam diameter and melting

Electron beam diameter d（mm）	10	20	30
Melting depth h1（mm）	5.71	8.99	9.98
Melting width h2（mm）	27.80	32.52	37.71

Under the condition that other conditions remain constant, the diameter of the electron beam is increased to observe the temperature field change of the titanium alloy, and it can be seen from Fig. 10, Fig. 11 and

Table **IV** that the increase of the diameter of the electron beam will gradually deepen the melting depth and the melting width will gradually widen. When the scanning speed is increased from 10mm to 30mm, the melting width increases from 27.80mm to 37.71mm, indicating that a reasonable increase in the diameter of the electron beam can make the raw material melt quickly and reduce the number of scans.

Effect of Electron Beam Acceleration Voltage on TC4 Melting Process

In order to study the influence of different electron beam acceleration voltages on the surface temperature field and the change of melting depth of titanium alloy during the melting process of titanium alloy, the temperature change of y=20mm plane (D=10mm) when the electron beam acceleration voltage is 20kv, 30kv, 40kv, and the midpoint of the electron beam moves to the (50, 20) point, respectively. And other process parameters of the electron beam used in the simulation are shown in

Table V:

Table V. Process parameters

Scanning speed v(mm/s)	**Electron beam diameter d(mm)**	**Voltage U(kv)**	**Current I(A)**	**Scanning spacing D(mm)**
20	10	—	5	10

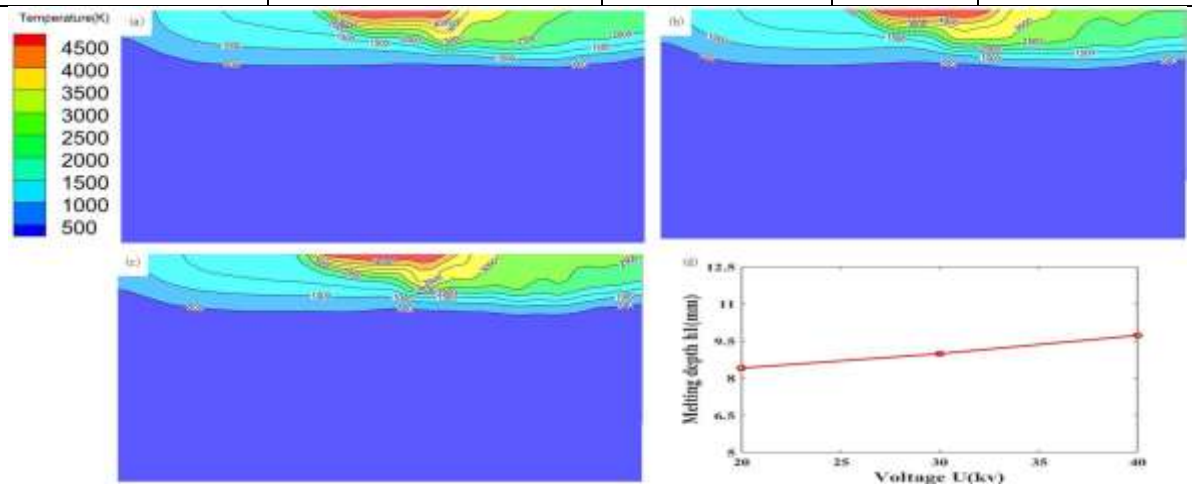

Fig. 12 Plane temperature diagram of y=20 mm (a)U=20kv (b)U=30kv (c)U=40kv

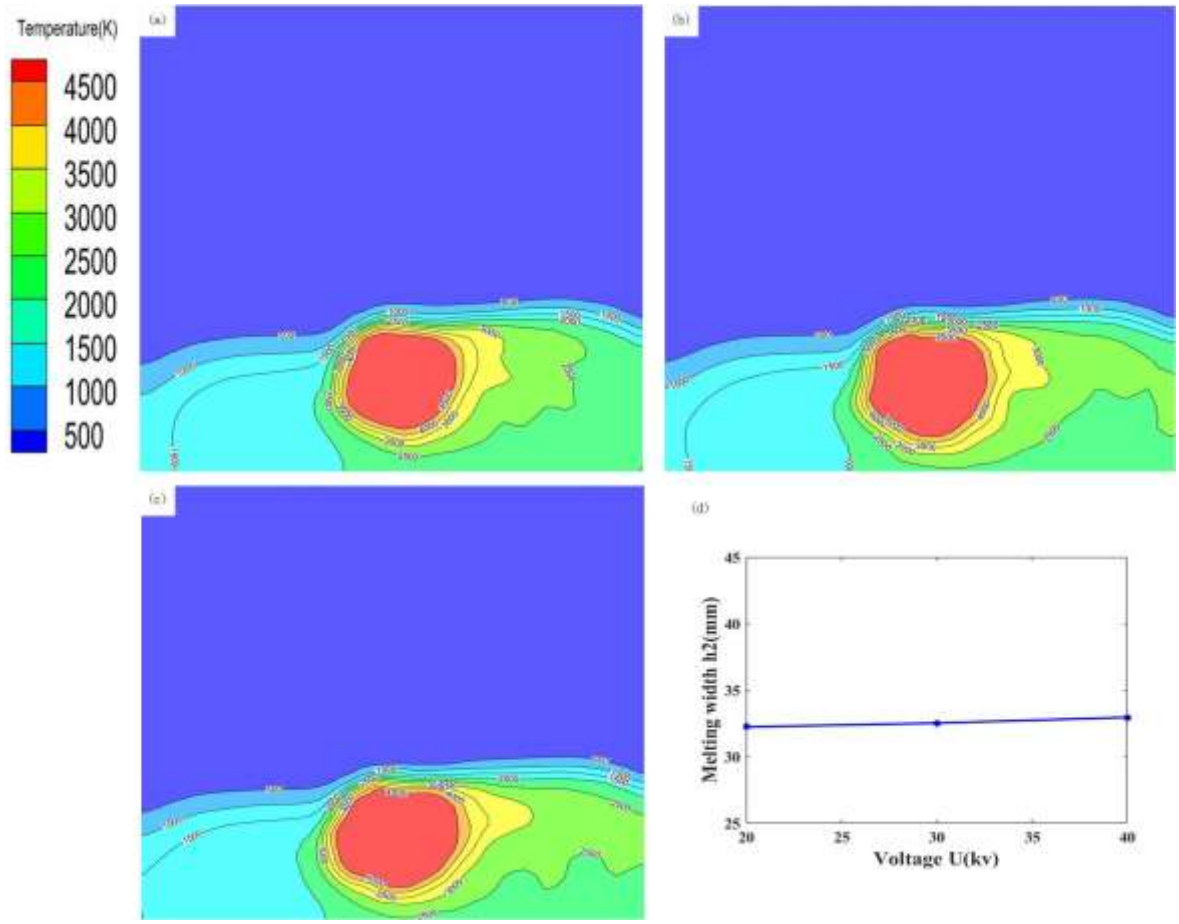

Fig. 13. Upper surface temperature map (a)U=20kv (b)U=30kv (c)U=40kv

Table VI. Relationship between acceleration voltage and melting

Voltage U(kv)	20	30	40
Melting depth h1(mm)	8.41	8.99	9.73
Melting width h2(mm）	32.23	32.52	32.95

Under the condition that other conditions remain constant, increasing the accelerating voltage of the electron beam and observing the temperature field change of the titanium alloy, it can be seen from Fig. 12, Fig. 13 and

Table VI that the increasing accelerating voltage of the electron beam will gradually deepen the melting depth and the melting width will gradually widen. Since the increase of the accelerating voltage will increase the surface temperature at this diameter, but the heat absorption capacity of the raw material is certain, the effect of the accelerating voltage on the melting process will not be obvious.

Effect of the current emitted by the electron beam on the TC4 melting process

In order to study the influence of the current[15] emitted by different electron beams on the surface temperature field of titanium alloy and the change of melting depth during the melting process of titanium alloy, the current of electron beam emission is 4A, 5A, 6A, and the temperature change of y=20mm plane (D=10mm) when the electron beam midpoint moves to (50, 20) point, respectively. And other process parameters of the electron beam used in the simulation are shown in :

Table VII. Process parameters

Scanning speed v(mm/s)	**Electron beam diameter d(mm)**	**Voltage U(kv)**	**Current I(A)**	**Scanning spacing D(mm)**

20	10	30	—	10

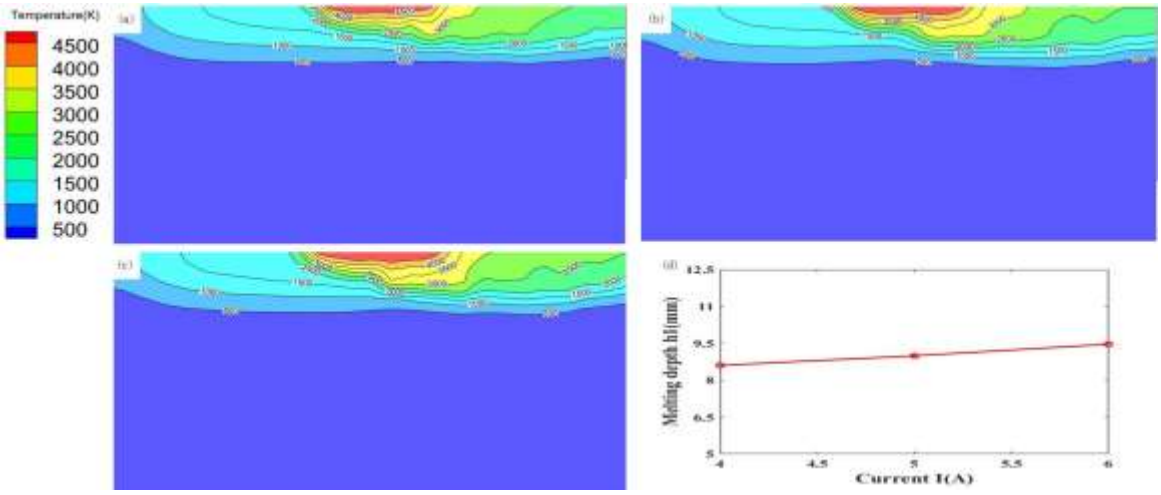

Fig. 14. Temperature diagram of y=20 mm plane (a)I=4A (b)I=5A (c)I=6A

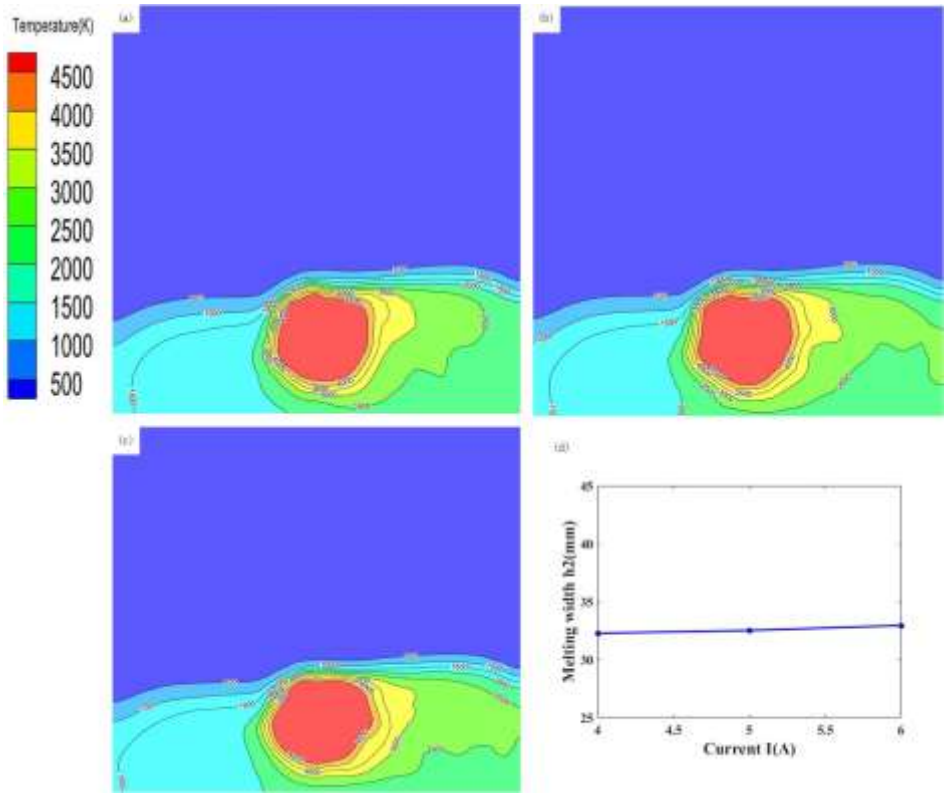

Fig. 15. Upper surface temperature chart (a)I=4A (b)I=5A (c)I=6A

Table VIII. Relationship between current and melting

Current I(A)	4	5	6
Melting depth h1(mm)	8.60	8.99	9.46
Melting width h2(mm）	32.28	32.52	33.38

Under the condition that other conditions remain constant, the current during the emission of the electron beam is increased, and the temperature field of the titanium alloy is observed, and the current at the time of the electron beam emission is increased to gradually deepen the melting depth and the melting width to gradually widen from

Fig. 14, Fig. 15 and

Table **VII. Process parameters**

Scanning speed v(mm/s)	**Electron beam diameter**	**Voltage U(kv)**	**Current I(A)**	**Scanning spacing D(mm)**

	d(mm)			
20	10	30	—	10

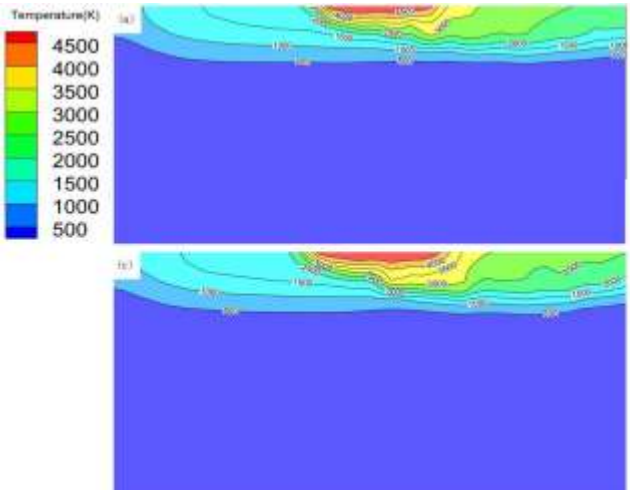

Fig. 14. Temperature diagram of y=20 mm plane (a)I=4A (b)I=5A (c)I=6A

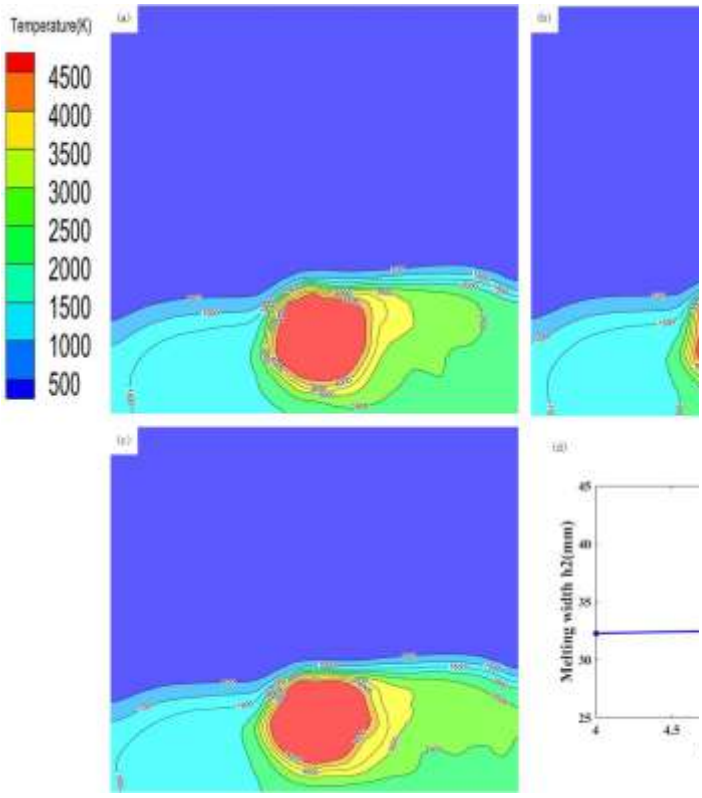

Fig. 15. Upper surface temperature chart (a)I=4A (b)I=5A (c)I=6A

Table VIII Since increasing the current emitted by the electron beam will increase the surface temperature at this diameter, but the heat absorption capacity of the raw material is certain, the effect of the accelerating voltage on the melting process will not be obvious.

Effect of the Spacing of the Electron Beam Scanning Trajectory on the TC4 Melting Process

In order to study the influence of the spacing of different electron beam scanning trajectories on the surface temperature field and the change of melting depth of titanium alloy during the melting process of titanium alloy, the temperature change of y=10+D mm plane when the spacing of electron beam scanning trajectories is 5mm, 10mm, 20mm, and the midpoint of the electron beam moves to the (50, 10+D) point, respectively. And other process parameters of the electron beam used in the simulation are shown in

Table **IX**:

Table IX. Process parameters

Scanning speed v(mm/s)	Electron beam diameter d(mm)	Voltage U(kv)	Current I(A)	Scanning spacing D(mm)
20	10	30	5	—

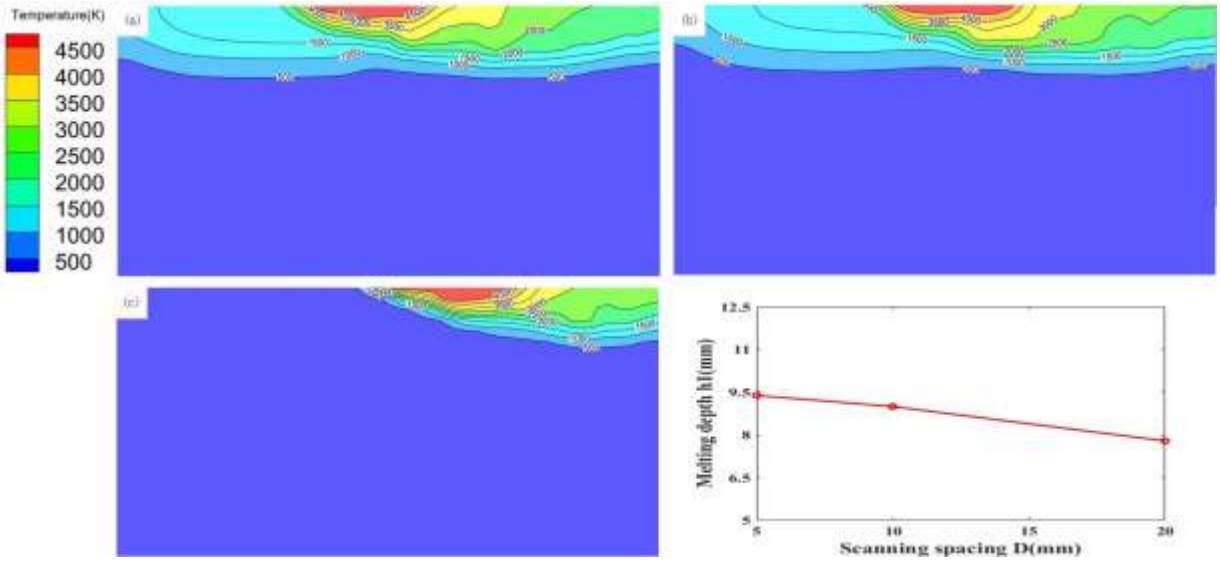

Fig. 16. Plane temperature plot of y=10+D mm (a)D=5mm (b)D=10mm (c)D=20mm

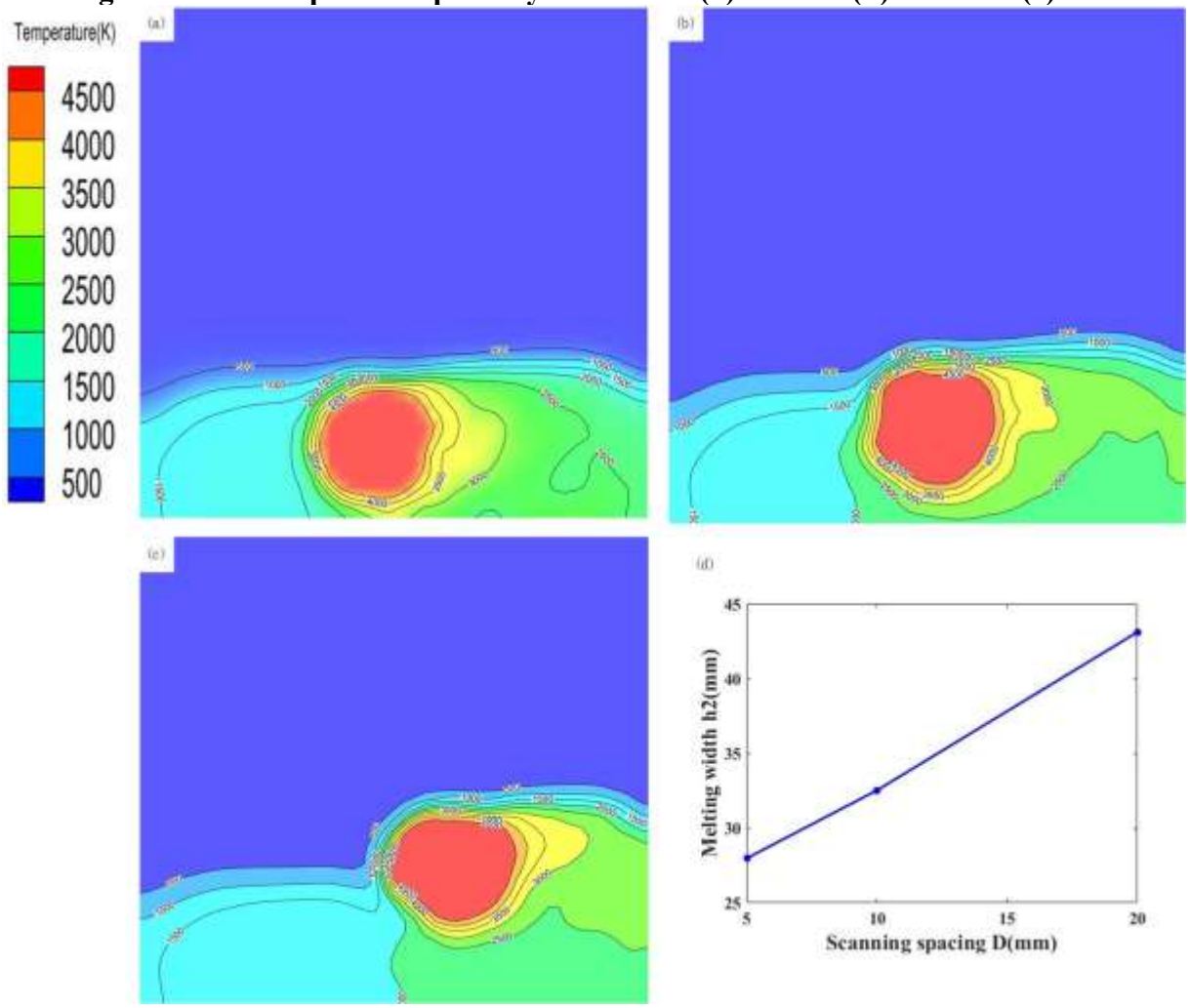

Fig. 17. Upper surface temperature map (a)D=5mm (b)D=10mm (c)D=20mm

Table X. Relationship between scan spacing and melting

Scanning spacing D(mm)		5		10		20
Melting depth h1（mm）		9.38		8.99		7.78
Melting width h2（mm）		27.97		32.52		43.11

Under the condition that other conditions remain unchanged, increase the scanning spacing of the electron beam and observe the temperature field change of the titanium alloy, and it can be concluded from Fig. 16, Fig. 17 and

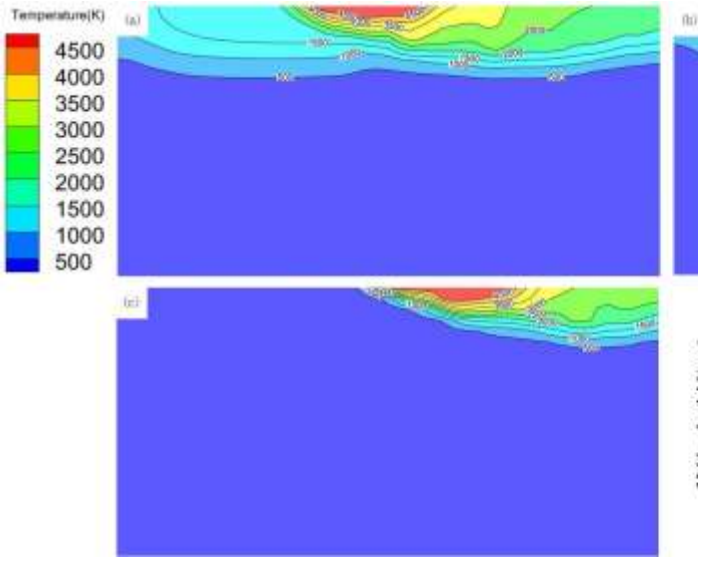

Fig. 16. Plane temperature plot of y=10+D mm (a)D=5mm (b)D=10mm (c)D=20mm

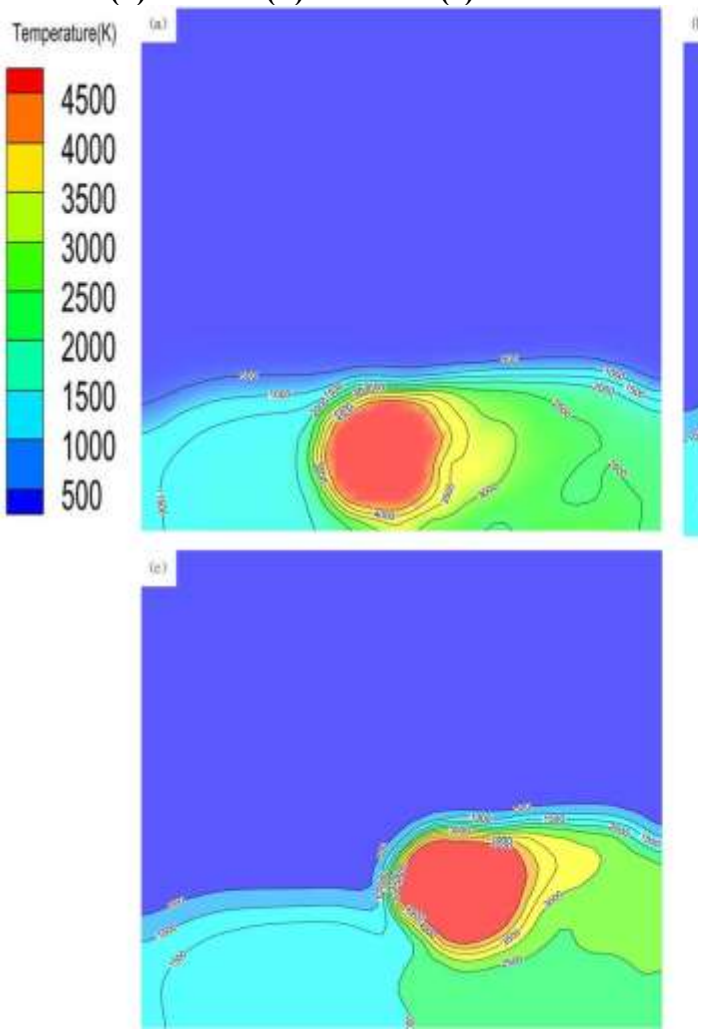

Fig. 17. Upper surface temperature map

(a)D=5mm (b)D=10mm (c)D=20mm

Table X that increasing the scanning spacing of the electron beam will gradually make the melting depth gradually shallower and the melting width gradually wider. When the scanning spacing increases from 5mm to 20mm, the melting depth decreases from 9.38mm to 7.78mm, and the melting width increases from 27.97mm to 43.11mm.

Conclusion

When melting titanium alloys in EB furnaces, increasing the scanning speed of the electron beam will significantly reduce the melting depth and width. Increasing the diameter of the electron beam deepens and widens the melting depth. Widening the scan spacing can slightly reduce the melting depth, but significantly broaden the melting width. The accelerating voltage and the current emitted by the electron beam have a limited effect on the melting due to their thermal saturation effect. The optimization strategy requires a combination of parameter adjustments, such as decreasing the speed, increasing the diameter or spacing, to increase the efficiency of a single melt and reduce the number of scans.

Conflict of interest statement

On behalf of all authors, the corresponding author states that there is no conflict of interest.

References

1. XC He, Yang Li, YJ Bi, XM Liu, B Zhou, SZ Zhang, SJ Li. Journal of Materials Science & Technology, 44 (09): 191-200(2020). https://doi.org/10.1016/j.jmst.2020.01.033.
2. H.R.Lashgari, M.Ferry, S.Li. Journal of Materials Science & Technology, 119 (24): 131-149(2022). https://doi.org/10.1016/j.jmst.2021.09.068
3. Y Wang, L Gao, Y Xin, S Guo, L Yang, H Ji, G Chen. Minerals, 14 (6): 601-601(2024). https://doi.org/10.3390/min14060601
4. L Gao, H Huang, Y Zhang, H Zhang, Z Shi, Y Jiang, R Zhou. JOM 70, 2934–2942 (2018). https://doi.org/10.1007/s11837-018-3048-0.
5. Körner C. *International Materials Reviews*, *61*(5), 361–377(2016). https://doi.org/10.1080/09506608.2016.1176289.
6. L Cao，L Zhang，RF Meng，QD Zhang.

Modelling and Simulation in Materials Science and Engineering, 30(3):034003(2022). https://doi.org/10.1016/j.jmapro.2020.07.025.
7. Hongxin L , Yefeng Y, Yang L, Feng L. Additive Manufacturing,50(1):102579(2022). https://doi.org/10.1016/j.addma.2021.102579.
8. Chaabene, A, Ben-Elechi, S, Chatti, S, Guerich M, Benkhalifa A. The International Journal of Advanced Manufacturing Technology, 135, 3865–3882 (2024). https://doi.org/10.1007/s00170-024-14731-0
9. Patel S, Vlasea M. Materialia, 9:100591(2020). https://doi.org/10.1016/j.mtla.2020.100591 .
10. J Jiang, Y Ding, X Qin, Y Zhang, Y Ke, J She, S Deng.. Diamond & Related Materials, 153 112099-112099(2025). https://doi.org/10.1016/j.diamond.2025.112099
11. Ping Y, Yunyi H, Riheng H, Junxi H, Meiyi C, Wenxiao Y, Kang Z. Metals, 15 (2): 168-168(2025). https://doi.org/10.3390/met1502 0168
12. Ning L, Tan Y, Wen S, Li P, You X, Wang X, Xuan W. Metallurgical and Materials Transactions, 54 (6): 2965-2984(2023). https://doi.org/10.1007/s11663-023-02881-7
13. Guilian W, Chuang W, Minke C, Xianglong L, Jinduo Y. Influence of scanning speed on spheroidization effect in electron beam selective melting[J]. Materials Today Communications, 41 111004-111004(2024). https://doi.org/10.1016/j.mtcomm.2024.111004
14. HS Jang, SH Kim, GW Park, JB Jeon, D Kim, Yoon Suk Choi, S Shin. Journal of Materials Research and Technology, 36 2938-2950(2025). https://doi.org/10.1016/j.jmrt.2025.03.272
15. S.A Teresa, F Simona, B Rosario, F Stefania, P Carmine, A Antonello.. Journal of Manufacturing Processes, 60 162-179(2020). https://doi.org/10.1016/j.jmapro.2020.10.065